Three-photon imaging of ovarian cancer

Jennifer Kehlet Barton*[a, b], Babak Amirsolaimani[b], Photini Rice[a], Kenneth Hatch[c], Khanh Kieu[b]
[a]Dept. of Biomedical Engineering, The Univ. of Arizona, 1657 E. Helen St. Tucson, AZ, USA 85721, [b]College of Optical Sciences, The Univ. of Arizona, 1630 E. University Blvd., Tucson, AZ, USA 85721, USA, [c]Dept. of Obstetrics and Gynecology, The Univ. of Arizona, 1501 N Campbell Ave, Tucson, AZ, USA 85724

ABSTRACT

Optical imaging methods have the potential to detect ovarian cancer at an early, curable stage. Optical imaging has the disadvantage that high resolution techniques require access to the tissue of interest, but miniature endoscopes that traverse the natural orifice of the reproductive tract, or access the ovaries and fallopian tubes through a small incision in the vagina wall, can provide a minimally-invasive solution.

We have imaged both rodent and human ovaries and fallopian tubes with a variety of endoscope-compatible modalities. The recent development of fiber-coupled femtosecond lasers will enable endoscopic multiphoton microscopy (MPM). We demonstrated two- and three-photon excited fluorescence (2PEF, 3PEF), and second- and third-harmonic generation microscopy (SHG, THG) in human ovarian and fallopian tube tissue. A study was undertaken to understand the mechanisms of contrast in these images. Six patients (normal, cystadenoma, and ovarian adenocarcinoma) provided ovarian and fallopian tube biopsies. The tissue was imaged with three-dimensional optical coherence tomography, multiphoton microscopy, and frozen for histological sectioning. Tissue sections were stained with hematoxylin and eosin, Masson's trichrome, and Sudan black.

Approximately 1 μm resolution images were obtained with an excitation source at 1550 nm. 2PEF signal was absent. SHG signal was mainly from collagen. 3PEF and THG signal came from a variety of sources, including a strong signal from fatty connective tissue and red blood cells. Adenocarcinoma was characterized by loss of SHG signal, whereas cystic abnormalities showed strong SHG. There was limited overlap of two- and three- photon signals, suggesting that three-photon imaging can provide additional information for early diagnosis of ovarian cancer.

Keywords: cancer, fallopian tube, multiphoton imaging, ovary, second harmonic generation, three-photon excited fluorescence, third harmonic generation, two-photon excited fluorescence

1. INTRODUCTION

1.1 Motivation

The fallopian tubes (FTs) are the location of serous tubal intraepithelial carcinoma (STIC), which is the putative precursor of most deadly ovarian cancers[1-3]. However, the FTs and ovaries are located deep within the body, and early, curable disease is manifest at a spatial scale well below the resolution of clinical whole-body techniques such as MRI, CT, or even vaginal ultrasound. No current screening technique (palpation, ultrasound or CA-125 blood marker) has been definitely shown to reduce death rates from ovarian cancer[4]. Therefore, women at high risk for ovarian cancer may be counseled to undergo prophylactic salpingo-oophorectomy as early as age 35[5], despite the fact that loss of fertility and sudden onset of post-menopause can be physically and psychologically challenging, and the procedure can increase cardiovascular mortality[6]. While the very high lifetime risk of ovarian cancer with a BRCA1 mutation (up to 70%[7]) means that salpingo-oophorectomy may be the most appropriate step for these women, for other women with less dramatic risk factors, the best action - as well as its timing - is unclear.

*barton@email.arizona.edu; phone 1 520 621-4116

Photonic Therapeutics and Diagnostics XII, edited by Bernard Choi, et al., Proc. of SPIE
Vol. 9689, 96893P · © 2016 SPIE · CCC code: 1605-7422/16/$18 · doi: 10.1117/12.2211798

Many women would benefit from a minimally-invasive, high resolution look at their FT and ovaries. The biggest beneficiaries may be pre-menopausal women with moderate-risk BRCA2 gene mutations, a moderate or strong family history of disease (e.g. one or more relatives with breast or ovarian cancer), or abnormal ultrasound or CA-125 results, but no other reason to go directly to surgery. These definitions encompass millions of women. The ready availability of genetic and CA-125 testing has increased knowledge but also anxiety among women. For example, despite CA-125 testing not being recommended as a diagnostic procedure, it is estimated that 50% of the 15 million tests performed in the year 2000 were for diagnostic purposes[8], a procedure with a 9.6% false positive rate[4].

1.2 Multiphoton microscopy

Multiphoton microscopy (MPM) is a relatively new imaging technology that has tremendous potential for both fundamental research and clinical diagnosis. Among the many submodalities available, two-photon excited fluorescence (2PEF)- in which two excitation photons are absorbed nearly simultaneously and fluorescence emission is at a wavelength shorter than excitation- offers increased depth of imaging and higher resolution over single photon imaging modalities such as confocal microscopy. Second harmonic generation (SHG), in which two photons combine in a scattering event to produce one photon at exactly half the incident wavelength, can provide exquisite maps of non-centrosymmetric molecules such as collagen. Three photon excited fluorescence (3PEF) and third harmonic generation (THG) imaging are less well studied but offer opportunities for even higher resolution imaging of a wide array of molecules[9-16]. Most commonly, ultrafast lasers based on Ti:Sapphire crystals are used, due to their high power, flexibility, and relative reliability. After about two decades of intensive development, MPM has found important applications in biological research, but has not yet made much of a foray into clinical practice. Two large and relatively expensive systems have been developed for skin imaging (DermaInspectTM and MPT-flex), which require an articulating arm and/or a motorized bed for the patient[17]. While these systems produce exquisite images, their complexity and price are obstacles to widespread use. Also, as femtosecond pulses suffer from pulse broadening in fiber optics, it has been challenging to develop flexible endoscopic delivery adding to the complexity of these systems, which use articulating arms or move the patient to the instrument. These systems illustrate the pressing need to reduce the large size, complexity, and cost of the current MPM laser sources. If the source problem can be resolved, MPM microscope optics themselves are simple- simpler than a confocal microscope- due to the confinement of the generated emission to a small volume, eliminating the need for descan detection and pinholes. Recently, there has been a strong push in research and development of fiber lasers for MPM[18-22]. They are becoming more and more powerful making them suitable for many MPM modalities. One author (Kieu) is an expert on new carbon nanotube saturable absorber technology that has enabled robust mode-locking in an all-fiber alignment-free laser design. He developed a 1550 nm laser and associated compact MPM system to be used in this study. The laser is smaller than a shoebox and the entire system occupies only a couple square feet of bench space.

1.3 Current study

The authors have extensive experience in imaging the human, rat and mouse ovary and FT with a variety of optical techniques. An *in vivo* study using laparoscopic optical coherence tomography (OCT) was able to clearly distinguish between normal vs. adenocarcinoma ovary, as well as several benign diseases[23]. A small follow up (9 patients/16 FTs) *ex vivo* study of FT tissue was recently performed. While there were no FT cancers, the difference between normal FT and salpingitis was clearly seen, as the inflamed tissue was characterized by loss of normal detailed tissue structure.

Similarly, the capacity to distinguish normal from cancerous ovarian tissue has been shown in hundreds of rodent ovaries using OCT and conventional bench top (Ti:Sapphire at 780 nm) MPM in a model of ovarian cancer[24-26]. Quantitative features (from Fourier and gray level co-occurrence matrix analysis) extracted from SHG images of 54 mice could be used to distinguish normal from cancer tissue with over 80% sensitivity and specificity[25]. 2PEF imaging has also proven to be useful, with analysis of 2PEF images obtained simultaneously with the SHG images showing statistically significant differences in particle size and number between normal and disease[26]. These studies have also shown that it is possible to detect intermediate stages of disease such as tubular adenoma, providing evidence that early detection can be possible. We have also performed in vivo, time serial imaging studies of mouse ovary[24]. In these studies, it was visualized how small punctate fluorescence in young, normal ovaries become large numerous dots in old, diseased ovaries, and the collagen fibers go from straight and collinear to tangled.

However, a study of three-photon contrast in ovary and FT has not previously been performed. Also, it is expected that the mechanisms of contrast at 1550 nm differ from those at 780 nm. We undertook a pilot study to examine the ability of OCT and MPM to visualize differences between normal and cancerous ovary and FT biopsies.

2. MATERIALS AND METHODS

2.1 Human ovary and fallopian tube samples

Under a protocol approved by the University of Arizona Institutional Review Board, six women undergoing salpingo-oophorectomy were consented to provide surgical discard tissue for this study. One or two samples of ovary tissue, and zero or one samples of FT tissue were obtained. Information on the tissue obtained is given in Table 1. Volunteers were also asked to complete a risk assessment questionnaire. One volunteer was deemed high risked based on a family history of breast cancer; she was also the only pre-menopausal volunteer. Clinical diagnosis was obtained for each volunteer, and is included in parentheses if it differs from the histologically-determined diagnosis of the particular tissue sample imaged for this study.

Table 1. Volunteer information and samples obtained.

Volunteer #	Age	Ovary	FT
1	69	Normal	Normal
2	71	Normal	Normal
3	78	Adenocarcinoma	none
4	67	Normal (endometrial cancer)	Normal
5	46	Normal (high risk)	Normal
6	65	Mucinous cyst borderline	none

Tissues were kept in cold saline and transported to author labs for imaging with OCT and MPM. After imaging, tissues frozen using isopentane pre-cooled in liquid nitrogen, then embedded in optimal cutting temperature compound in cryomolds. Cryosectioning was performed, producing 5 μm thick tissue sections.

2.2 OCT Imaging

OCT imaging was performed with a tabletop, commercially swept-source OCT system (OCS1050SS, Thorlabs, Newton, NJ, USA), which has a central wavelength of 1040 nm and spectral bandwidth 80 nm which produced an axial resolution of 12 μm in air. The lateral resolution was approximately 12 nm. The A-scan rate of the system was 16 kHz. Three-dimensional image cubes were obtained with 512 (axial) x 750 (lateral in both x and y) voxels, covering an extent of 4 x 4 mm lateral and 2 mm in depth. Images presented are virtually re-sliced in the *en face* (parallel to the surface of the tissue) direction to correspond to the *en face* MPM images.

2.3 MPM Imaging

A diagram of the MPM system used in this study is shown in Figure 1. The fiber-coupled, very compact source has the following parameters (out of the fiber): center wavelength of 1560 nm, pulse duration of 150 fs, 8 MHz repetition rate, 40 mW average power. The light is scanned with galvo-scanning mirrors through a set of lenses and a 20x, 0.5 NA objective onto the tissue. A lateral resolution of 1.1 μm is achieved. Images with 1000 x 1000 pixels are obtained in approximately 2 s. Remitted light is deflected with a dichroic beam splitter and separated into two channels. In the presented images, these are coded red for 2PEF and SHG, and green for 3PEF and THG. Presented images are approximately 1.1 mm x 1.1 mm in extent.

The following mechanisms of contrast were expected for the MPM images. 2PEF has a single photon correspondence of approximately 775 nm. There are no appreciable endogenous fluorophores at this wavelength so negligible 2PEF is expected. SHG is fairly wavelength independent. From previous studies by us and others, this signal is known to be primarily from collagen in ovary tissue. 3PEF has a single photon correspondence of approximately 516 nm. At this green wavelength metabolic co-factors such as NADH and FAD should fluoresce, as should lipopigments, especially lipofuscin. THG is know to occur at interfaces and optical heterogeneities, and may be expected at lipids.

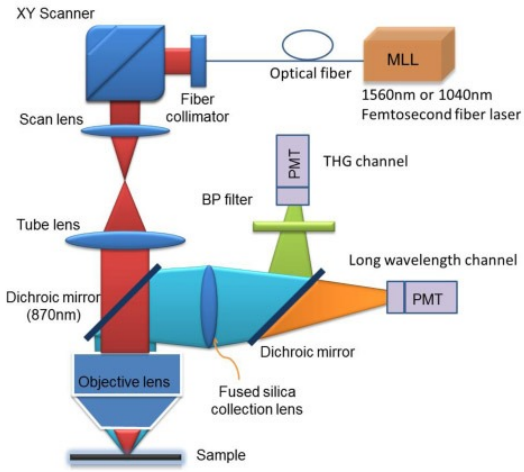

Figure 1. Block diagram of the MPM system used in this study.

2.4 Histology

Frozen sections of the tissue were stained with hematoxylin and eosin (H&E, standard anatomical stain), Masson's trichrome (collagen stains blue, connective tissue pink, and nuclei purple), and Sudan Black (lipids stain black). Images were obtained of the slides on a brightfield microscope at 10x magnification, providing a comparable field of view (1 x 1.4 mm) to the MPM images.

3. RESULTS AND DISCUSSION

3.1 Clear sources of contrast

Some MPM images were clear as to the source of contrast. Two example MPM images of FT are given in Figure 2. The left image shows a trail of green dots which were clearly identified in this and other images as being THG generated by red blood cells, likely because of the strong optical discontinuity between the plasma and the red blood cell and well as resonance enhancement with the hemoglobin. The wavy fibular red strands are very similar to SHG signal seen from collagen in previous studies. The diffuse, dimmer green signal is likely 3PEF from cellular metabolic co-factors. The origin of the single green dots is less clear- they may be single red blood cells from a vessel caught in cross-section, or other strong punctate source of discontinuity such as lipid droplets. The right image shows strong SHG from connective tissue, and very strong THG and possibly 3FEP from fatty connective tissue that could be seen by the eye.

3.2 Normal ovary MPM, OCT, and histology

Figure 3 shows an image sequence of MPM, H&E, Trichrome, and Sudan black histology, and OCT of normal ovary from a pre-menopausal volunteer. The OCT image (4 x 4 mm) is approximately 4x the scale of the other images (MPM 1.1 x 1.1 mm and histology 1 x 1.4 mm) in each dimension. The MPM image (top left) taken near the surface of the tissue shows abundant red SHG from organized collagen, some faint diffuse green 3PEF, and punctate green signal, possibly from red blood cells or fatty droplets. The H&E image (center top) confirms abundant collagen stained pink. The Masson's trichrome histology (top right) is mostly blue-stained collagen, with some potentially fluid-filled clear spaces that are about the same size and shape as signal voids in the MPM image. The Sudan Black image shows many moderately-sized lipofuscin granules stained black. The green dots in the MPM image are much smaller, so they are probably not caused by lipofuscin fluorescence. The OCT image (bottom left) is a snapshot of the volume at approximately 200 μm depth. A swirling pattern likely caused by reflectance from the collagen structure is evident. In this pre-menopausal ovary, a developing follicle with egg is also seen in the upper left of the image.

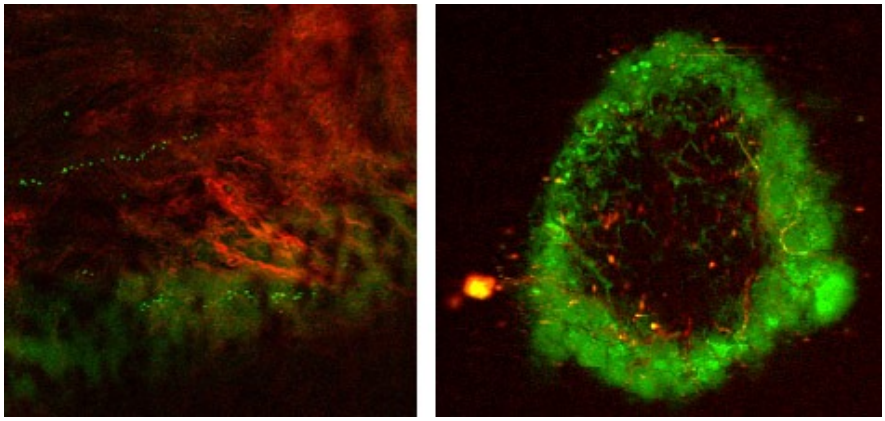

Figure 2. (Left) normal fallopian tube MPM image showing a trail of punctate green THG from red blood cells, diffuse green 3PEF from cellular metabolic co-factors, and wavy linear red SHG from organized collagen fibers. (Right) red and green SHG and THG from connective tissue, green THG and possibly 3PEF from fat.

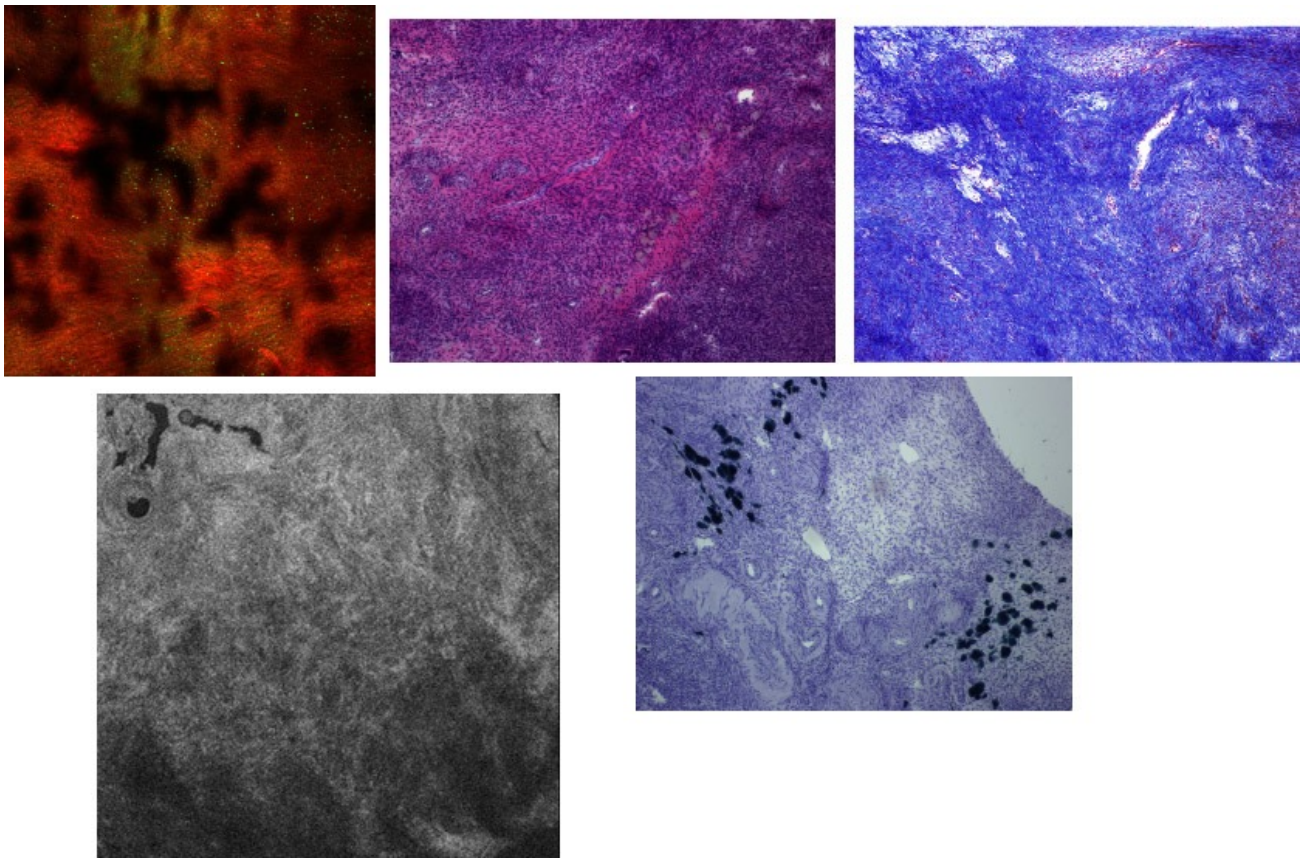

Figure 3. (Top left) normal ovary MPM image, H&E histology image (center top), Masson's trichrome histology image (top right), Sudan black histology image (bottom right) and OCT image (bottom left). OCT image is 4 x 4 mm, MPM is 1.1 x 1.1 mm, histology to MPM scale.

Figure 4 shows an image sequence for an ovary with adenocarcinoma. Diffuse green 3PEF is seen, possibly from metabolically active cancer mass, with abundant punctate green THG. Almost no SHG signal is seen, indicating a lack of organized collagen. This status is confirmed with the H&E showing only loose pink collagen, and limited blue on the

Masson's trichrome image. The collagen that is present appears wispy and unorganized. The Sudan black histology image shows nothing of interest. The OCT image echoes the disordered appearance.

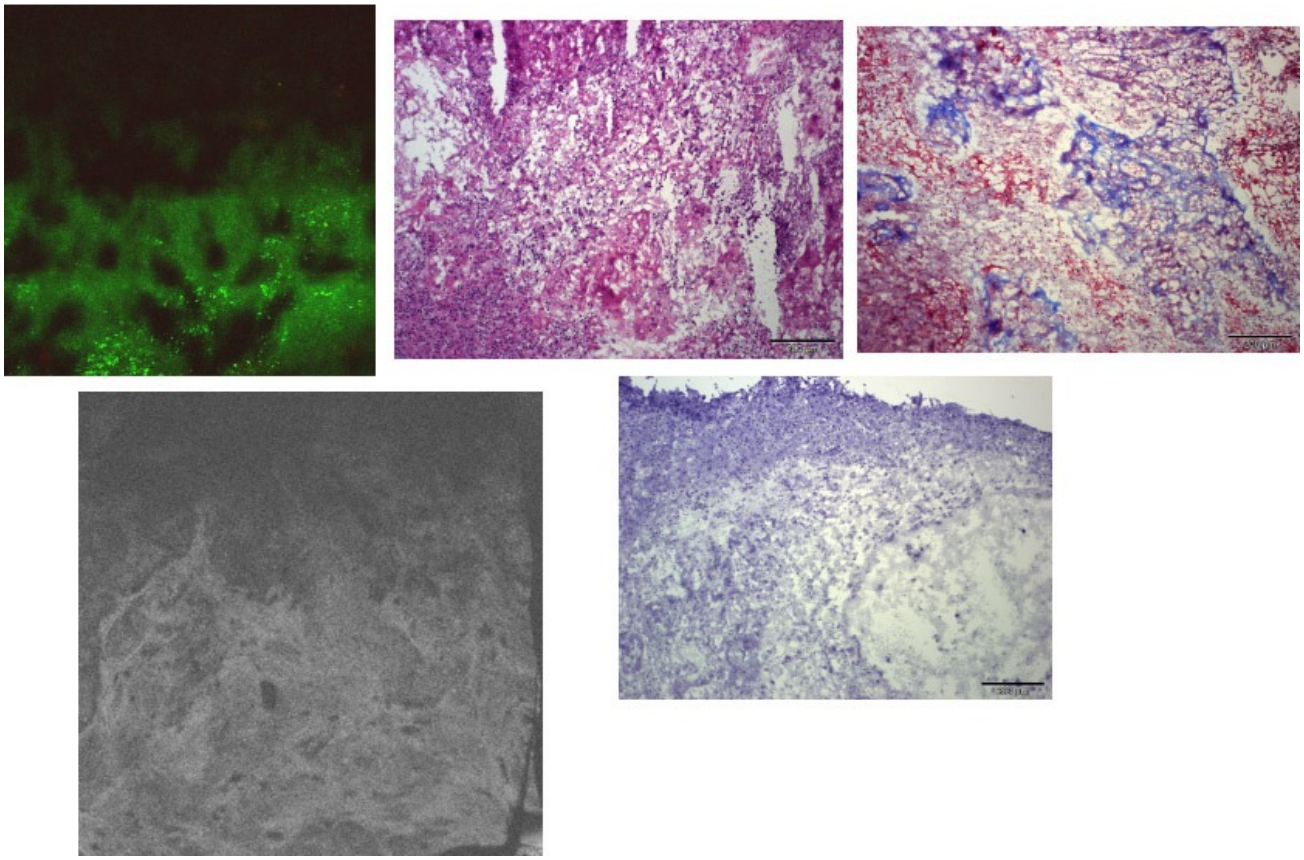

Figure 4. (Top left) adenocarcinoma ovary MPM image, H&E histology image (center top), Masson's trichrome histology image (top right), Sudan black histology image (bottom right) and OCT image (bottom left). OCT image is 4 x 4 mm, MPM is 1.1 x 1.1 mm, histology to MPM scale.

In contrast, an image set from an ovary with mucinous cystadenoma is shown in Figure 5. Here, a very strong red SHG signal is seen, likely from the tightly packed collagen of the cyst wall. Very limited three-photon signal is seen. The H&E histology image appears to show ropy pink collagen strands, and the Masson's trichrome histology image confirms thick blue collagen surrounding the cysts. Again the Sudan black image is unremarkable, with no lipofuscin seen.

4. CONCLUSION

This study confirms, as seen in previously, that SHG is outstanding for visualizing organized collagen. This signal was abundant in normal ovary and cystic abnormalities, and lessened or absent in adenocarcinoma. It also provides some insight into the origin of three-photon (3PEF and THG) signal in the ovaries and FTs. 3PEF appears much weaker than THG, and is probably from the metabolic co-factors NADH/FAD. Although it was expected that 3PEF signal would be generated form lipofuscin, the strong punctate signal seen did not correlate with black-stained lipopigment granules seen on Sudan black histology. It is possible the fluorescence was simply too weak to be apparent with our imaging protocol. THG appears to be generated from red blood cells and fatty connective tissue. The alternative histology stains of Masson's trichrome and Sudan black were extremely helpful for understanding the tissue components.

There were some limitations to this study. There were only 6 patients/15 samples studied, and only one adenocarcinoma and one benign cystadenoma. While orientation was carefully maintained, it is extremely difficult to assure that MPM images, OCT images, and frozen sections are obtained from the same location. Particularly in the abnormal tissues, a

great deal of heterogeneity was seen in the tissue, and a misregistration of a few millimeters can affect interpretation. Future work includes studying additional samples and some instrumentation enhancements. First, we would like to perform imaging with a 1300 nm fiber source which can be used for both (co-registered) OCT and MPM. This shorter wavelength will excite more fluorophores- potentially porphyrins with 2PEF, and more strongly excite NADH in 3PEF. Also, since it was sometimes unclear whether the three-photon signal came from 3PEF or THG, we plan to increase the number of detectors to separate the harmonic generation from fluorescence.

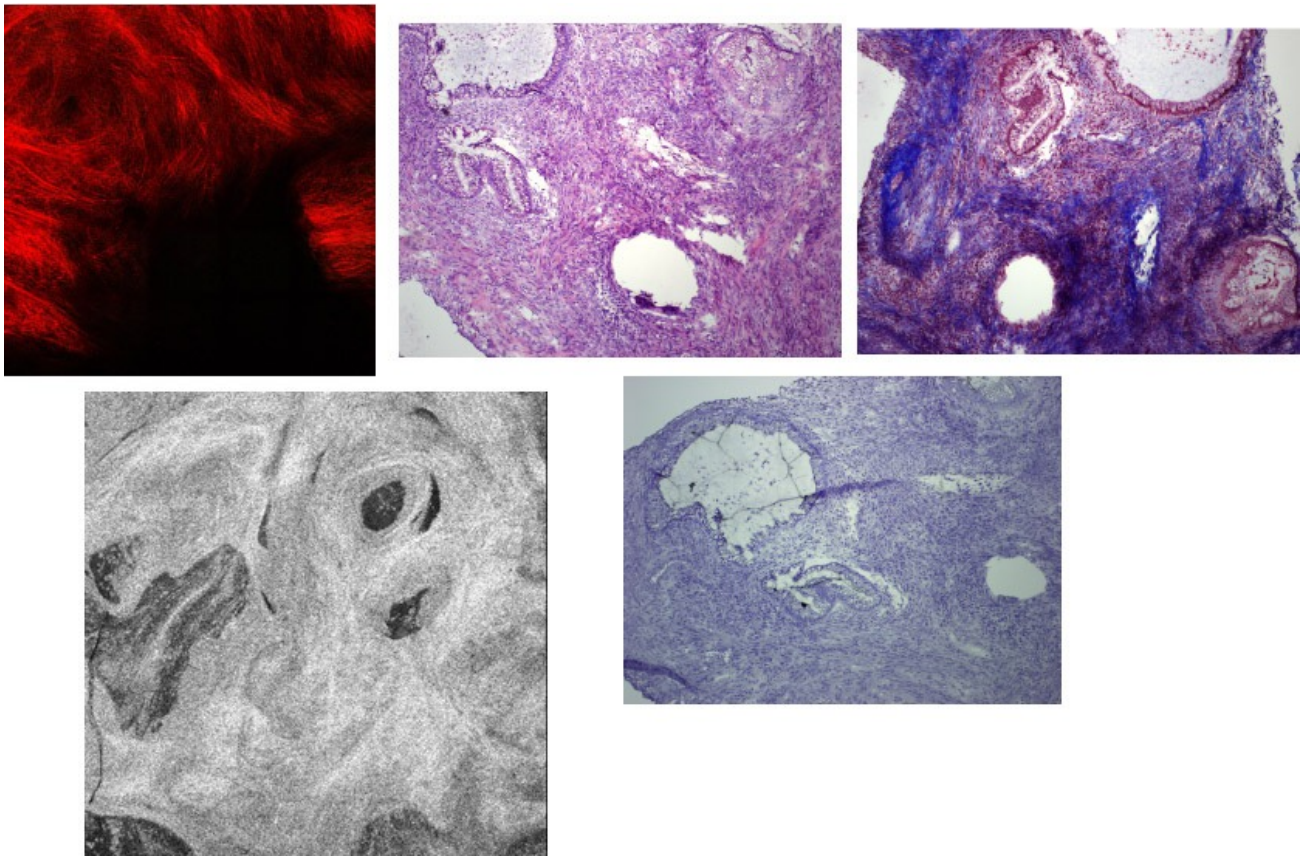

Figure 5. (Top left) adenocarcinoma ovary MPM image, H&E histology image (center top), Masson's trichrome histology image (top right), Sudan black histology image (bottom right) and OCT image (bottom left). OCT image is 4 x 4 mm, MPM is 1.1 x 1.1 mm, histology to MPM scale.

REFERENCES

[1] Kurman, R.J., Shih, I.M., "The Origin and Pathogenesis of Epithelial Ovarian Cancer: A Proposed Unifying Theory," Am. J. Surg. Pathol. 34, 433-443, (2010).

[2] Kuhn, E., Kurman, R.J., Shih, I.M., "Ovarian cancer is an imported disease: Fact or fiction?," Curr. Obstet. Gynecol. Rep. 1, 1-9, (2012).

[3] Vang, R., Shih, L., Kurman, R.J., "Fallopian tube precursors of ovarian low- and high-grade serous neoplasms," Histopathology 62, 44-58, (2013).

[4] Buys, S.S., "Ovarian cancer screening in the Prostate, Lung, Colorectal and Ovarian (PLCO) cancer screening trial: Findings from the initial screen of a randomized trial," Am. J. Obstet. Gynecol. 193, 1630-1639, (2005).

[5] Finch, A.P.M., Lubinski, J., Møller, P.I., Singer, C.F., Karlan, B., Senter, L., Rosen, B., Maehle, L., Ghadirian, P., Cybulski, C., Huzarski, T., Eisen, A., Foulkes, W.D., Kim-Sing, C., Ainsworth, P,. Tung, N., Lynch, H.T., Neuhausen, S., Metcalfe, K.A., Thompson, I., Murphy, J., Sun, P., Narod, S.A., "Impact of Oophorectomy on

Cancer Incidence and Mortality in Women With a BRCA1 or BRCA2 Mutation," J. Clinical Oncology 32(15), 1547-53, (2014).
[6] Rivera CM, Grossardt BR, Rhodes DJ, Brown RD, Roger VL, Melton J, Rocca WA, "Increased cardiovascular mortality following early bilateral oophorectomy," Menopause 16, 15-23, (2009).
[7] American Cancer Society, "Cancer Facts and Figures 2015," (2015).
[8] Frantz Medical Group "LPL Technologies," http://www.frantzgroup.com/fmv/portfolio/lpl.html, (2005).
[9] Denk W, Strickler J H, Webb W W, "Two-photon laser scanning fluorescence microscopy," Science 248, 73-76, (1990).
[10] König K, "Multiphoton microscopy in life sciences," J. Microsc. 200, 3–104, (2000).
[11] Juergen C. Jung and Mark J. Schnitzer, "Multiphoton endoscopy," Opt. Lett. 28, 902-904, (2003).
[12] Zipfel W, Williams R, Webb W W, "Nonlinear magic: Multiphoton microscopy in the biosciences," Nature Biotechnol. 21, 1369-1377, (2003).
[13] Helmchen F, Denk W, "Deep tissue two-photon microscopy," Nat. Methods 2, 932-940, (2005).
[14] Kobat D, Horton NG, Xu C, "In vivo two-photon microscopy to 1.6-mm depth in mouse cortex," J. Biomed. Opt. 16, 106014, (2011).
[15] Erich E, Hoover J, Squier A, "Advances in multiphoton microscopy technology," Nature Photonics 7, 93-101, (2013).
[16] Nicholas G, Horton, Wang K, Kobat, D Clark CG, Wise FW, Schaffer CB, Xu C, "In vivo three-photon microscopy of subcortical structures within an intact mouse brain," Nature Photonics 7, 205-209, (2013).
[17] Koenig K, "Multiphoton multimodal tomography of in vivo human skin," IntraVital 1(1):1-26, (2012).
[18] Millard AC, Wiseman PW, Fittinghoff DN, Wilson KR, Squier JA, Müller M, "Third-harmonic generation microscopy by use of a compact, femtosecond fiber laser source," Appl. Opt. 38(36), 7393-7397, (1999).
[19] Kieu K, Saar BG, Holtom GR, Wise FW, Xie XS, "High power all-fiber picosecond laser system for Coherent Raman Microscopy," Opt. Lett. 34, 2051-2053, (2009).
[20] Liu G, Kieu K, Wise FW, Chen Z, "Multiphoton Microscopy System with a Compact Fiber-based Femtosecond-pulse Laser and Handheld Probe," Journal of Biophotonics, 4, 34-39, (2011).
[21] Nie B, Saytashev I, Chong A, Liu H, Arkhipov SN, Wise FW, Dantus M, "Multimodal microscopy with sub-30 fs Yb fiber laser oscillator," Biomed. Opt. Express 3, 1750-1756, (2012).
[22] Wise, FW, "Femtosecond Fiber Lasers Based on Dissipative Processes for Nonlinear Microscopy," Selected Topics in Quantum Electronics, IEEE Journal 18, 1412-1421, (2012).
[23] Hariri LP, Bonnema GT, Schmidt K, Winkler AM, Korde V, Hatch KD, Davis JR, Brewer MA, Barton JK, "Laparoscopic optical coherence tomography imaging of human ovarian cancer," Gynecologic Oncology, 114, 188-194, (2009).
[24] Watson JM, Marion SL, Rice PF, Bentley DL, Besselsen DG, Utzinger U, Hoyer PB, Barton JK, "In vivo time-serial multi-modality optical imaging in a mouse model of ovarian tumorigenesis," Cancer Biol. Ther. 15, 42-60, (2014).
[25] Watson JM, Rice PF, Marion SL, Brewer MA, Davis JR, Rodriguez JJ, Utzinger U, Hoyer PB, Barton JK, "Analysis of second-harmonic-generation microscopy in a mouse model of ovarian carcinoma," J. Biomed. Opt. 17, 076002, (2012).
[26] Watson JM, Marion SL, Rice PF, Utzinger U, Brewer MA, Hoyer PB, Barton JK, "Two-photon excited fluorescence imaging of endogenous contrast in a mouse model of ovarian cancer," Lasers Surg. Med. 45, 155-166, (2013).